

ORIGINAL ARTICLE

Effects of bFGF on suppression of collagen type I accumulation and scar tissue formation during wound healing after mucoperiosteal denudation of rat palate

WOOKJIN CHOI¹, HITOSHI KAWANABE¹, YOSHIHIKO SAWA²,
KUNIHISA TANIGUCHI³ & HIROYUKI ISHIKAWA¹

¹Section of Orthodontics, Department of Oral Growth & Development, Division of Clinical Dentistry, Fukuoka Dental College, Japan, ²Section of Functional Structure, Department of Morphological Biology, Division of Biomedical Science, Fukuoka Dental College, Japan and ³Section of Pathology, Department of Morphological Biology, Division of Biomedical Sciences, Fukuoka Dental College, Japan

Abstract

Objective. The purpose of this study was to evaluate the effect of basic fibroblast growth factor (bFGF) on collagen changes after mucoperiosteal denudation of rat palate. **Material and methods.** A total of 36 male Wistar rats were divided into control, scar, sham, and bFGF groups. In the scar, sham, and bFGF groups, lateral palatal mucoperiosteum was excised to form scar tissue on the palate. In the bFGF group, bFGF solution was injected into the operated area 1 week postoperatively. At 6 weeks postoperatively, the distribution of collagen type I and the 3-dimensional structure of collagen fibers were investigated under immunofluorescent and scanning electron microscopy. **Result.** In the bFGF group, weakly immunostained submucosa was clearly distinguishable from the strongly immunostained cervical periodontal ligament and gingiva. Collagen fibers running from submucosal tissue into the surface of underlying palatal bone comprised loosely arranged collagen fibrils. Lumen structures in collagen fibers resembled those in the control group. **Conclusion.** Administration of bFGF for suppression of collagen type I generation could suppress scar tissue formation and reduce connective strength with adjacent teeth and palatal bone.

Key Words: Basic fibroblast growth factor, cleft palate, collagen fiber, collagen type I, scar formation

Introduction

Almost all surgical procedures to close a palatal cleft result in mucoperiosteal denudation of bone [1]. However, postoperative wound contraction and scar tissue formation inhibit normal maxillary growth and dento-alveolar development [2,3]. Palatal scar tissue formation finally ends in the development of collagen-rich tissue, mainly comprising collagen type I fibers, which may contribute to the rigidity of scar tissue [4,5]. Leenstra et al. [6] reported that after palatal mucoperiosteal denudation healed in beagle dogs, collagen fibers inserting into the raw palatal bone surface from scar tissue remained thickened and firmly connected, thus inhibiting maxillary growth. Gimi et al. [7] reported that in the healing process of rat palatal wounds, collagen fibers become buried in the regenerated bone, and a

massive collagenous layer is closely attached to the bone surface.

Recently, in an attempt to reduce wound contraction and scar formation induced by mucoperiosteal denudation, we investigated the effects of basic fibroblast growth factor (bFGF) as a pharmaceutical modulator of the wound healing process [8,9]. Studies have identified bFGF as a biological mediator that regulates connective tissue cell migration, proliferation and synthesis of intracellular protein and extracellular matrix [10–12]. *In vivo* studies have demonstrated that topical application of exogenous bFGF enhances the healing process following bone fracture [13] and facilitates periodontal regeneration in surgically created furcation Class II defects [14,15]. *In vitro* studies have identified bFGF as an inducer of vascular endothelial growth factor

(VEGF), thus promoting angiogenesis through VEGF expression [16,17].

In our previous studies, after bFGF administration on rat palates in the early wound-healing stage, less lingual inclination of molars and greater maxillary vertical growth were seen compared to non-treated animals from postoperative week 6 [8]. The histological results suggested that bFGF reduces the collagen content of subsequently formed scar tissue [8]. Scanning electron microscopy (SEM) showed that bFGF improved vascular supply to the operated mucosa and underlying bone during palatal wound healing [9].

The present study evaluated whether bFGF administration affects collagen type I distribution and structure of collagen fiber after mucoperiosteal denudation in rat palate. This may confirm that bFGF administration after cleft palate surgery with mucoperiosteal denudation can suppress postoperative scar tissue formation, leading to more favorable maxillary growth.

Material and methods

Animals

A total of 36 male Wistar rats (mean weight, 50 g) were used in this study at 20 days old. All animals were kept under normal laboratory conditions and provided with *ad libitum* access to standard rat chow and water. The experiment was approved by the Board for Animal Experiments at Fukuoka Dental College. Animals were divided into 4 groups ($n=9$ each): control, scar, sham, and bFGF groups. In each group, 5 animals were used for histological preparation and 4 for cell-maceration/SEM [18]. No significant differences in weight were seen among the 4 groups throughout the experimental period.

Surgical procedure of scar formation and bFGF injection

In the scar, sham and bFGF groups, mucoperiosteum was removed from the palate in accordance with the methods described by Kim et al. [19]. Rectangular strips of the bilateral one-third of hard palatal mucoperiosteum were excised under general anesthesia induced by intraperitoneal injection of $7 \text{ mg} \cdot \text{kg}^{-1}$ of sodium pentobarbital (Nembutal; Abbott Laboratories, Chicago, Ill., USA). The greater palatine neurovascular bundles were not avulsed during the operation. The exposed bone surface was wiped with a cotton pellet for complete removal of the periosteum (Figure 1). Control animals did not undergo any surgical procedure.

Recombinant bFGF was provided by Kaken Pharmaceutical (Tokyo, Japan). In the bFGF group, $10 \mu\text{L}$ of bFGF solution ($20 \mu\text{g}$ bFGF/ $10 \mu\text{L}$ distilled water) was injected into each side of the operated area using a syringe (Hamilton, Reno, Nev., USA) at



Figure 1. Schematic of rat palatal mucoperiosteal denudation. Rectangle indicates surgically operated areas. Asterisks show sites of injection.

1 week postoperatively. The sham group received an injection of $10 \mu\text{L}$ of distilled water.

At 6 weeks postoperatively, animals were carefully anesthetized by intraperitoneal injection of $7 \text{ mg} \cdot \text{kg}^{-1}$ of sodium pentobarbital (Nembutal; Abbott Laboratories, Chicago, Ill., USA) after performing inhalation anesthesia with ether. A polyethylene catheter tube was introduced into the aorta for perfusion.

Histological preparation

After perfusion, the maxilla was removed, immersed in 10% formalin, decalcified in 10% EDTA, dehydrated in a graded series of ethanol, and embedded in paraffin. Serial frontal sections of $7 \mu\text{m}$ thickness were taken around the disto-lingual root of the 1st molar for hematoxylin and eosin (HE) staining and immunofluorescent staining.

Immunofluorescent staining of collagen type I

After deparaffinization and dehydration, sections were treated with 0.05% collagenase (Wako Pure Chemical Industries, Osaka, Japan) for 10 min at 37°C in a culture dish containing moistened filter paper to provide humidity, then rinsed off with phosphate-buffered saline (PBS). Sections were then blocked in 1% goat normal serum (Vector Laboratories, Burlingame, Calif., USA) for 30 min at room temperature. After washing with PBS,

sections were incubated with $2 \mu\text{g} \cdot \text{ml}^{-1}$ of rabbit anti-rat collagen type I polyclonal antibody (Chemicon, Temecula, Calif., USA) for 12 h in 4°C . Following an additional wash with PBS, sections were incubated with Alexa flour 488 conjugated goat anti-rabbit IgG (Probes Invitrogen, Eugene, Oreg., USA) for 60 min at room temperature and washed again with PBS. Finally, sections were mounted with mounting media and observed under fluorescence microscopy (LSM-GB200; Olympus, Tokyo, Japan).

SEM procedure

We employed the cell-maceration method to clarify the 3-dimensional architecture of collagen fibrils, particularly collagen fibrillar networks abutting on the palatal bone surface (Figure 2). Cell-macerated specimens were prepared according to the method described by Ohtani et al. [18]. Specimens were macerated in 2 N NaOH at room temperature for 4 days, eliminating cellular elements and exposing connective tissue fibers effectively and consistently. After washing in distilled water for 3 days, specimens were placed in 2% tannic acid for 3 h, rinsed in distilled water for several hours, and postfixed in a 1% OsO_4 for 1 h. Specimens were dehydrated in series of graded concentrations of ethanol, and critical point-dried using liquid CO_2 . Dried specimens were mounted on metal stubs, coated with platinum (SEM coating Unit E5150 Poralon Equipment Ltd., Watford, England), and observed under SEM (JSM-6330F; JEOL, Tokyo, Japan).

Results

Light microscopic investigation

Control group. The mucoperiosteum comprises 4 distinct layers: epithelium, lamina propria, submu-

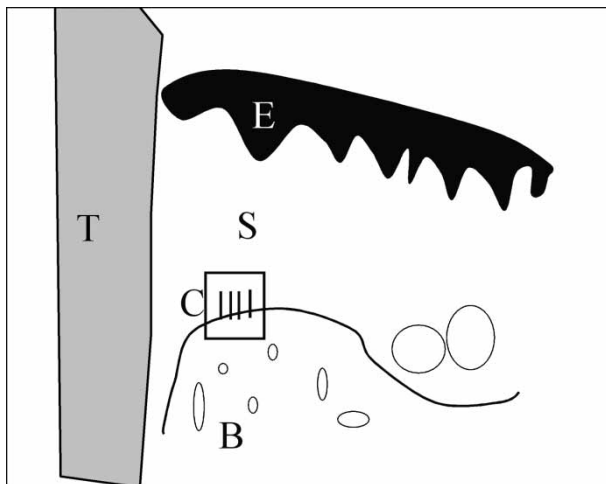


Figure 2. Area of SEM observation. C = collagen fibers running from submucosal tissue into underlying palatal bone surface; T = tooth; B = palatal bone; S = submucosa; E = epithelium.

cosa, and periosteum. The submucosa of the mucoperiosteum contains the major arteries, veins, and nerves of the palate. Beneath the epithelium, networks of coarse collagen fibers were apparent in staining using HE (Figure 3A).

Reactivity for collagen type I was strongly distributed throughout the cervical periodontal ligament, gingiva, lamina propria and periosteum, and was weakly distributed in the submucosa after immunofluorescent staining. Weakly immunostained submucosa was clearly distinguishable from the strongly immunostained cervical periodontal ligament and gingiva (Figure 4A).

Scar group. Scar tissue was clearly distinguishable from the normal mucoperiosteum. Thick bundles of collagen fibers were observed throughout the entire wound area in HE staining (Figure 3B).

Reactivity for collagen type I was more strongly distributed in the submucosa than that of the control group on immunofluorescent staining. Strongly immunostained submucosa was continuous with that of the cervical periodontal ligament and gingiva (Figure 4B).

Sham group. No histological differences were found in collagen bundles or distribution of collagen type I between sham and scar groups (Figure 3C, 4C).

bFGF group. Loosely woven collagen fibers were observed in the submucosal layer of the mucoperiosteum on HE staining (Figure 3D).

Reactivity for collagen type I was more weakly distributed in the submucosa than seen for the scar and sham groups under immunofluorescent staining. Weakly immunostained submucosa was clearly distinguishable from strongly immunostained cervical periodontal ligament and gingiva (Figure 4D).

Ultramicroscopic investigation

Collagen fibers were observed on SEM running from submucosal tissue into the surface of the underlying palatal bone. In the control group, collagen fibers mainly comprised loosely arranged collagen fibrils (Figure 6A). Lumens in collagen fibers displayed hemispherical and ovoid shapes (Figure 5A).

In the scar and sham groups, collagen fibers comprised densely arranged fibrillar structures (Figure 6B, C). Lumen structure as seen in the control group was not identified (Figure 5B, C).

In the bFGF group, collagen fibers comprised loosely arranged collagen fibrils (Figure 6D). Lumens in collagen fibers resembled those for the control group (Figure 5D).

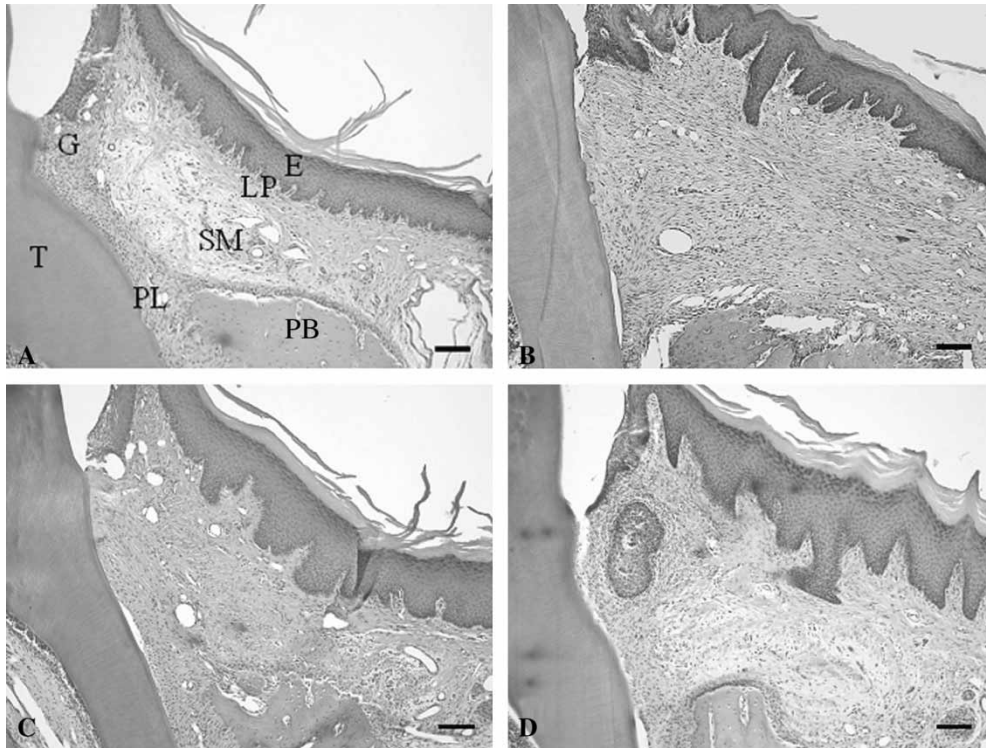


Figure 3. HE staining showing a frontal section of the rat palate at postoperative week 6 (A = control group; B = scar group; C = sham group; D = bFGF group). Scale bars represent 100 μ m. E = epithelium; LP = lamina propria; SM = submucosa; G = gingiva; PB = palatal bone; T = 1st molar tooth; PL = periodontal ligament.

Discussion

In the present study, the experimental duration and method of bFGF administration were determined on the basis of previous studies [8,9]. The dose of

bFGF was 20 μ g per side of the operated area. This bFGF administration was performed at one location and just once after re-epithelialization in palatal wounds, that is, 1 week after excision, with the expectation of minimizing adverse effects from

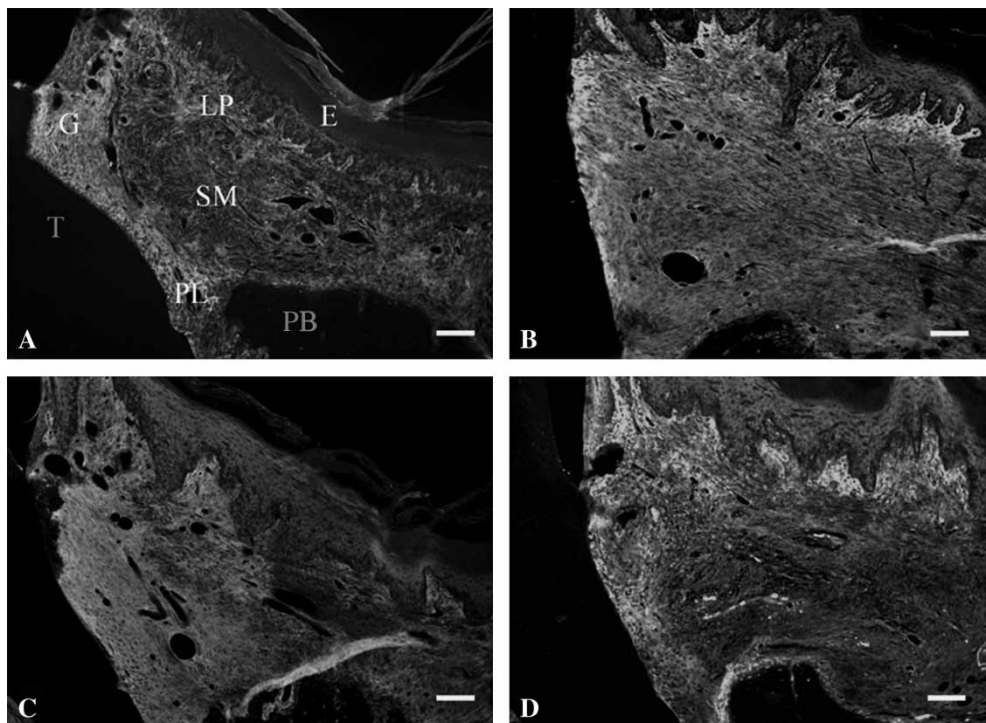


Figure 4. Immunofluorescent staining of collagen type I showing serial frontal section of HE staining in Figure 3 (A = control group; B = scar group; C = sham group; D = bFGF group). Scale bars represent 100 μ m.

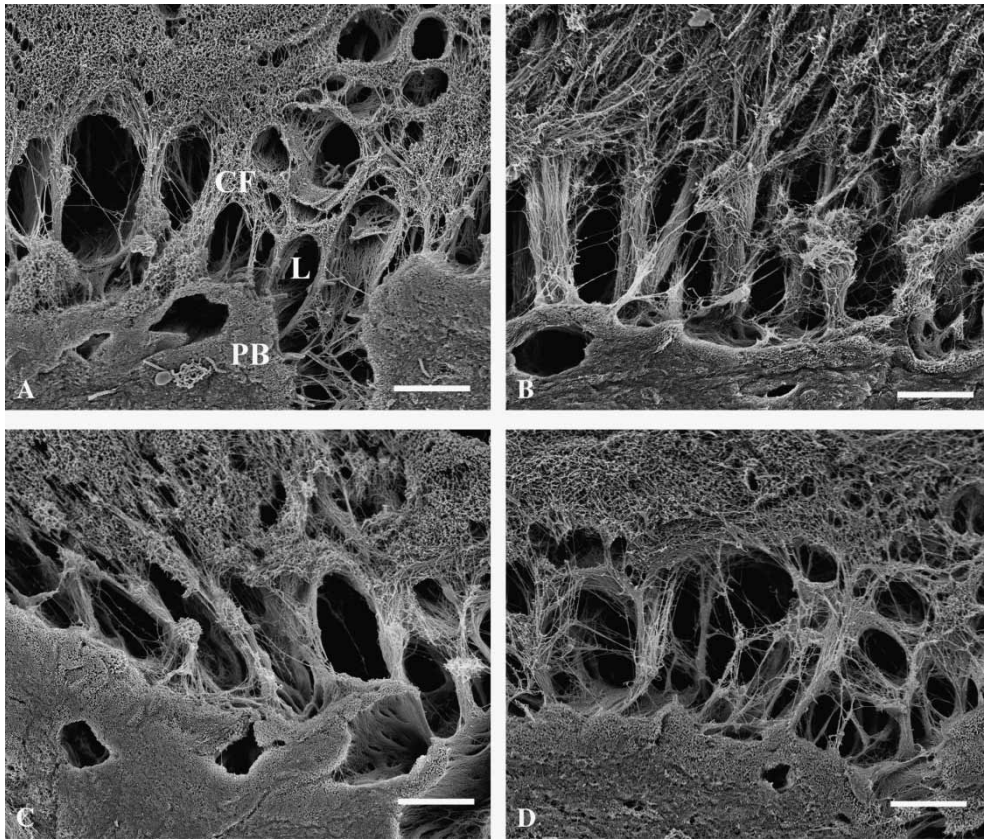


Figure 5. Scanning electron micrographs showing collagen fibers running from submucosal tissue into underlying palatal bone surface at postoperative week 6. In the bFGF group, lumens in collagen fibers resemble those in the control group (A = control group; B = scar group; C = sham group; D = bFGF group). Scale bars represent 10 μm . L = lumen; CF = collagen fiber; PB = palatal bone.

injection. However, the dose of bFGF and timing of injection are considered to greatly influence the results. Dose-dependency and optimal timing of the injection should be investigated in further studies.

Studies have examined the efficacy of bFGF on collagen synthesis and degradation related to fibroblast differentiation. The bFGF enhances proliferative responses of immature fibroblasts, stimulates collagenase gene expression, and suppresses differentiation of immature fibroblast [20,21]. Immature fibroblasts express more bFGF receptors than differentiated fibroblast [20]. These findings support the possible contribution of bFGF to regulating the extracellular matrix during wound healing.

In this study, examination under light microscopy showed that bFGF administration during the early wound-healing stage induces a significant reduction in collagen type I within the submucosal area (Figure 4D). These findings suggest that bFGF may suppress the differentiation of immature fibroblast, resulting in suppression of scar tissue formation.

In scar and sham groups, the tight connective tissue displaying strong immunostaining for collagen type I in the submucosa was continuous with that in the cervical periodontal ligament and gingiva (Figure 4B, C). Mature scar tissue in a growing animal might thus induce a medially directed tensile force on the teeth, resulting in narrowing of the

dental arch [2,6]. In the bFGF group, soft connective tissue that stained weakly for collagen type I in the submucosa was clearly distinguishable from that in the cervical periodontal ligament and gingiva (Figure 4D). It is thought that bFGF may reduce the insertion of collagen fibers from cervical periodontal ligament and gingiva into the submucosal area. Administration of bFGF may therefore contribute to reductions in mutual connective strength and subsequent relief of growth inhibition.

Collagen fibers between the scar tissue and raw palatal bone surface are also considered a cause of growth inhibition, as these fibers can remain thickened and firmly connected [7]. Thick collagen fibers are embedded in the palatal bone, creating a rigid attachment between scar tissue and underlying bone during palatal wound healing [2,6,7,22]. The present study clearly demonstrated the 3-dimensional structure of collagen fiber networks on the palatal bone surface [18]. In scar and sham groups, structures of collagen fibers between scar tissue and the underlying palatal bone surface comprised densely gathered fibrils. Lumen structure as seen in the control group was not identified (Figure 5B, C, 6B, C). However, collagen fibers in the bFGF group comprised loosely gathered fibrils, and lumens were recognizable between collagen fibers. These structures resembled those in the control group

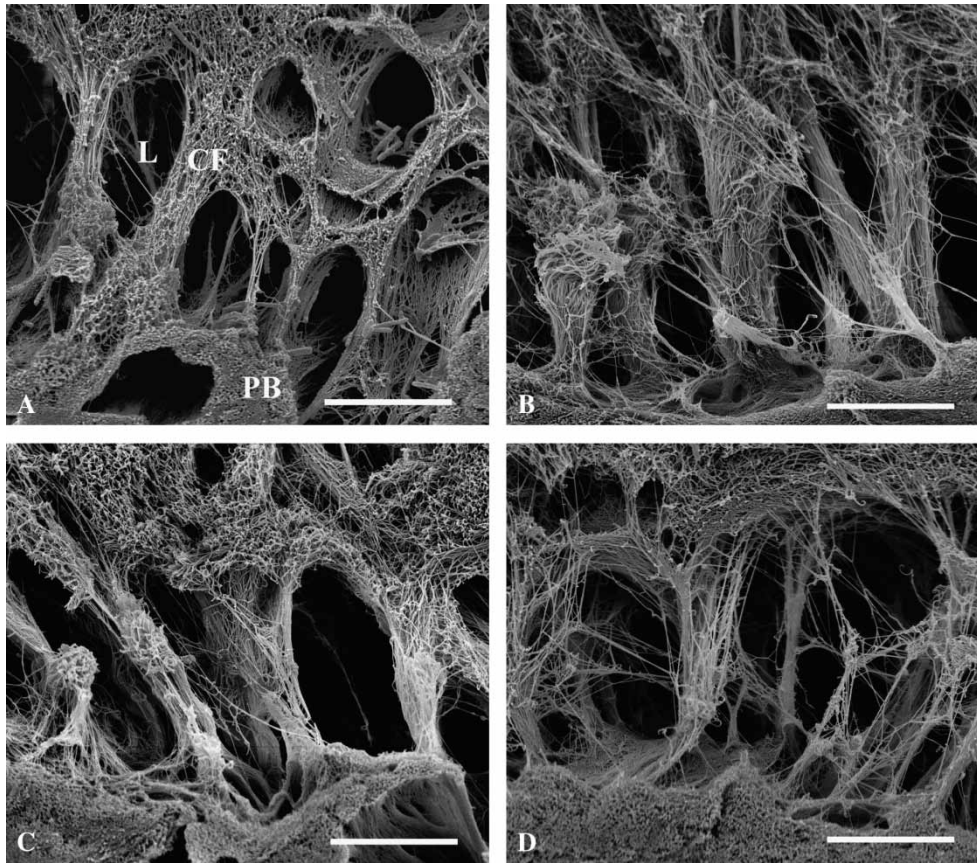


Figure 6. Scanning electron micrography showing collagen fibers from Figure 5. Collagen fibers in the bFGF group comprise loosely arranged collagen fibrils, similar to those seen in the control group (A = control group; B = scar group; C = sham group; D = bFGF group). Scale bars represent 10 μ m.

(Figure 5A, D, 6A, D). There were a number of lumens in the control and bFGF group. Because the lumen is considered of cell space, it is thought that bFGF may enhance regeneration of the periosteum and prevent the embedding of collagen fibers by palatal bone deposition.

Our previous studies have shown that bFGF can improve vascular supply in palatal wound healing [9], which may suggest that bFGF stimulates capillary proliferation and contributes to nutrient supply for the proliferation of immature fibroblasts. In conclusion, bFGF suppressed collagen type I generation and subsequent scar tissue formation, reducing connective strength with the adjacent teeth and palatal bone. Use of bFGF may thus lead to more favorable dento-alveolar growth after cleft palate surgery with mucoperiosteal denudation. To establish growth factor therapy for cleft palate surgery, clinical trials are currently ongoing to determine the safety and efficacy of bFGF administration [23,24].

Acknowledgments

We thank the Kaken Pharmaceutical Co., Ltd, Tokyo, Japan for supplying bFGF for this experiment.

References

- [1] Meng T, Shi B, Lu DW, Li Y, Wu M. Roles of palatine bone denudation repairing with free buccal or palatal mucosal graft on maxillary growth: an experimental study in rabbits. *Ann Plast Surg* 2007;59:323–8.
- [2] Wijdeveld MG, Maltha JC, Gruppig EM, De Jonge J, Kuijpers-Jagtman AM. A histological study of tissue response to simulated cleft palate surgery at different ages in beagle dogs. *Arch Oral Biol* 1991;36:837–43.
- [3] Ishikawa H, Nakamura S, Misaki K, Kudoh M, Fukuda H, Yoshida S. Scar tissue distribution on palates and its relation to maxillary dental arch form. *Cleft Palate Craniofac J* 1998; 35:313–9.
- [4] Cornelissen AM, Stoop R, Von den Hoff HW, Maltha JC, Kuijpers-Jagtman AM. Myofibroblasts and matrix components in healing palatal wounds in the rat. *J Oral Pathol Med* 2000;29:1–7.
- [5] Stadelmann WK, Digenis AG, Tobin GR. Physiology and healing dynamics of chronic cutaneous wounds. *Am J Surg* 1998;176:26–38.
- [6] Leenstra TS, Maltha JC, Kuijpers-Jagtman AM, Spauwen PH. Wound healing in beagle dogs after palatal repair without denudation of bone. *Cleft Palate Craniofac J* 1995; 32:363–9.
- [7] Gimi H, Sunakawa H, Arakaki K, Hiratsuka H. A histological study on healing process of palatal wound with bone denudation. *J Jpn Cleft Palate Assoc* 1998;23:214–25.
- [8] Kawanabe H, Ishikawa H, Kinoshita S, Taniguchi K. Short communication: Effects of basic fibroblast growth factor administration on wound healing process of rat palates with scar tissue formation. *Dent Jpn (Tokyo)* 2005;41:75–7.

- [9] Hata Y, Kawanabe H, Hisanaga Y, Taniguchi K, Ishikawa H. Effects of basic fibroblast growth factor administration on vascular changes in wound healing of rat palates. *Cleft Palate Craniofac J* 2007;45:63–72.
- [10] Heldin CH, Westermark B. Growth factors: mechanism of action and relation to oncogenes. *Cell* 1984;37:9–20.
- [11] Hauschka PV, Mavrakos AE, Iafrafi MD, Doleman SE, Klagsbrun M. Growth factors in bone matrix. Isolation of multiple types by affinity chromatography on heparin-Sepharose. *J Biol Chem* 1986;261:12665–74.
- [12] Wahl SM, Wong H, McCartney-Francis N. Role of growth factors in inflammation and repair. *J Cell Biochem* 1989;40:193–9.
- [13] Kawaguchi H, Kurokawa T, Hanada K, Hiyama Y, Tamura M, Ogata E, et al. Stimulation of fracture repair by recombinant human basic fibroblast growth factor in normal and streptozotocin-diabetic rats. *Endocrinology* 1994;135:774–81.
- [14] Takayama S, Murakami S, Shimabukuro Y, Kitamura M, Okada H. Periodontal regeneration by FGF-2 (bFGF) in primate models. *J Dent Res* 2001;80:2075–9.
- [15] Murakami S, Takayama S, Kitamura M, Shimabukuro Y, Yanagi K, Ikezawa K, et al. Recombinant human basic fibroblast growth factor (bFGF) stimulates periodontal regeneration in class II furcation defects created in beagle dogs. *J Periodontal Res* 2003;38:97–103.
- [16] Ribatti D, Nico B, Vacca A, Roncali L, Presta M. Endogenous and exogenous fibroblast growth factor-2 modulate wound healing in the chick embryo chorioallantoic membrane. *Angiogenesis* 1999;3:89–95.
- [17] Seghezzi G, Patel S, Ren CJ, Gualandris A, Pintucci G, Robbins ES, et al. Fibroblast growth factor-2 (FGF-2) induces vascular endothelial growth factor (VEGF) expression in the endothelial cells of forming capillaries: an autocrine mechanism contributing to angiogenesis. *J Cell Biol* 1998;141:1659–73.
- [18] Ohtani O, Ushiki T, Taguchi T, Kikuta A. Collagen fibrillar networks as skeletal frameworks: a demonstration by cell-maceration/scanning electron microscope method. *Arch Histol Cytol* 1988;51:249–61.
- [19] Kim T, Ishikawa H, Chu S, Handa A, Iida J, Yoshida S. Constriction of the maxillary dental arch by mucoperiosteal denudation of the palate. *Cleft Palate Craniofac J* 2002;39:425–31.
- [20] Takayama S, Murakami S, Miki Y, Ikezawa K, Tasaka S, Terashima A, et al. Effects of basic fibroblast growth factor on human periodontal ligament cells. *J Periodontal Res* 1997;32:667–75.
- [21] Pickering JG, Ford CM, Tang B, Chow LH. Coordinated effects of fibroblast growth factor-2 on expression of fibrillar collagens, matrix metalloproteinases, and tissue inhibitors of matrix metalloproteinases by human vascular smooth muscle cells. Evidence for repressed collagen production and activated degradative capacity. *Arterioscler Thromb Vasc Biol* 1997;17:475–82.
- [22] Leensta TS, Kuijpers-Jagtman AM, Maltha JC. The healing process of palatal tissues after palatal surgery with and without implantation of membranes: an experimental study in dogs. *J Mater Sci Mater Med* 1998;9:249–55.
- [23] Tanigawa T, Nakayama M, Nakamura T, Inafuku S. Use of trafermin to treat a skin ulcer after repair of a deep auricular laceration: a case report. *J Dermatolog Treat* 2005;16:345–6.
- [24] Motomura H, Ohashi N, Harada T, Muraoka M, Ishii M. Aggressive conservative therapy for refractory ulcer with diabetes and/or arteriosclerosis. *J Dermatol* 2006;33:353–9.